Preprints of the 21st IFAC World Congress (Virtual)
Berlin, Germany, July 12-17, 2020

Rijke Organ: Modeling and Control of Array of Rijke Tubes

Krištof Pučejdl Zdeněk Hurák Jiří Zemánek

Faculty of Electrical Engineering,
Czech Technical University in Prague, CZ
{*kristof.pucejdl, hurak, jiri.zemanek*}*@fel.cvut.cz*

Abstract: Rijke tube is a popular physical experiment demonstrating a spontaneous generation of sound in an open vertical pipe with a heat source. This laboratory instance of thermoacoustic instability has been researched due to its significance in practical thermoacoustic systems. We revisit the experiment, focusing on the possible use of the Rijke tube as a musical instrument. The novelty presented in this paper consists in shifting the goal from sound suppression to active sound generation. This called for modifying the previously investigated methods for stabilization of thermoacoustic oscillations into their excitation and control of their amplitude. On our way towards this goal, we developed a time-domain mathematical model that considers the nonlinear and time-varying aspects of the Rijke tube. The model extends the existing modeling and analysis approaches, which are mainly based in frequency domain. We also present an extension of the basic laboratory setup in the form of an array of Rijke tubes equipped with a single speaker used to control multiple Rijke tubes with different natural frequencies simultaneously.

Keywords: Rijke tube, Rijke organ, System modeling, Thermoacoustic instability, Time-delay systems

1. INTRODUCTION

Discovered in 1859 by a Dutch physicist Petrus Leonardus Rijke, a static source of heat—as simple as a wire mesh preheated with a burner—placed inside a vertically oriented open pipe gives rise to a loud humming noise. The sound goes away once the pipe is turned horizontally, but it reappears as soon as it is turned upright again. As such, the Rijke tube is an acoustically attractive experiment that catches attention and is often used as a demonstration during popular science lectures. As documented by Raun et al. (1993), numerous configurations exist, but there have not been many published attempts to exploit the underlying physical phenomenon other than by suppressing it. In this paper, we propose using the Rijke tube as the base principle for a musical instrument—*Rijke organ*.

Previous developments in understanding, modeling and control of Rijke tube were predominantly motivated by its close relation to practical systems that tend to develop thermoacoustic oscillation: engines, furnaces, and various combustion systems in general. The ultimate goal in a vast majority of such applications is to suppress these undesirable oscillations, that is, to *stabilize the system*. Active control of thermoacoustic (combustion) instabilities by means of a feedback was researched in 1980s. These early developments were documented by McManus et al. (1993) and Candel (1992). Heckl (1988) appears to be one of the first to study feedback stabilization based on frequency-domain analysis of the system. Later years witnessed application of advanced control techniques such as Campos-Delgado et al. (2003) who applied the $\mathcal{H}_\infty$ disturbance rejection and loopshaping techniques. More recently, Epperlein et al. (2015) used a similar setup to further investigate and describe the problem and compare experimental results with a system modal description. Besides the active control approaches, passive stabilization techniques have also been enjoying renewed interest of researchers recently: Zalluhoglu and Olgac (2018) show the possibility of passive stabilization by an acoustic resonator mounted onto the Rijke tube.

For our application, we can also benefit from suppression (e.g., for muting the tone), but more importantly, we need to control the oscillations in terms of the rise time and magnitude control. Such requirements do not allow us to use the many simplifying assumptions that are proven valid for simple suppression tasks. In particular, it is no longer possible to restrict the analysis to the frequency domain only. Many of the secondary phenomena in the Rijke tube, such as the dynamics of the buoyancy-driven air convection or the dynamics of the heat transfer and dissipation, affect the performance significantly and they have a nonlinear character. Therefore, we constructed a time-domain model of the Rijke tube that captures the main aspects of the nonlinear long-period dynamics and allows for numerical simulations of the system. We implemented the simulation models using MATLAB and Simulink.

2. MATHEMATICAL MODEL OF RIJKE TUBE DYNAMICS

Our model considers a Rijke tube system portrayed in the schematic drawing in Fig. 1a. An open glass tube is equipped with a microphone, an electrically powered wire heater element, and a loudspeaker. The former is used as a sensor, the latter two are used to generate

Copyright lies with the authors

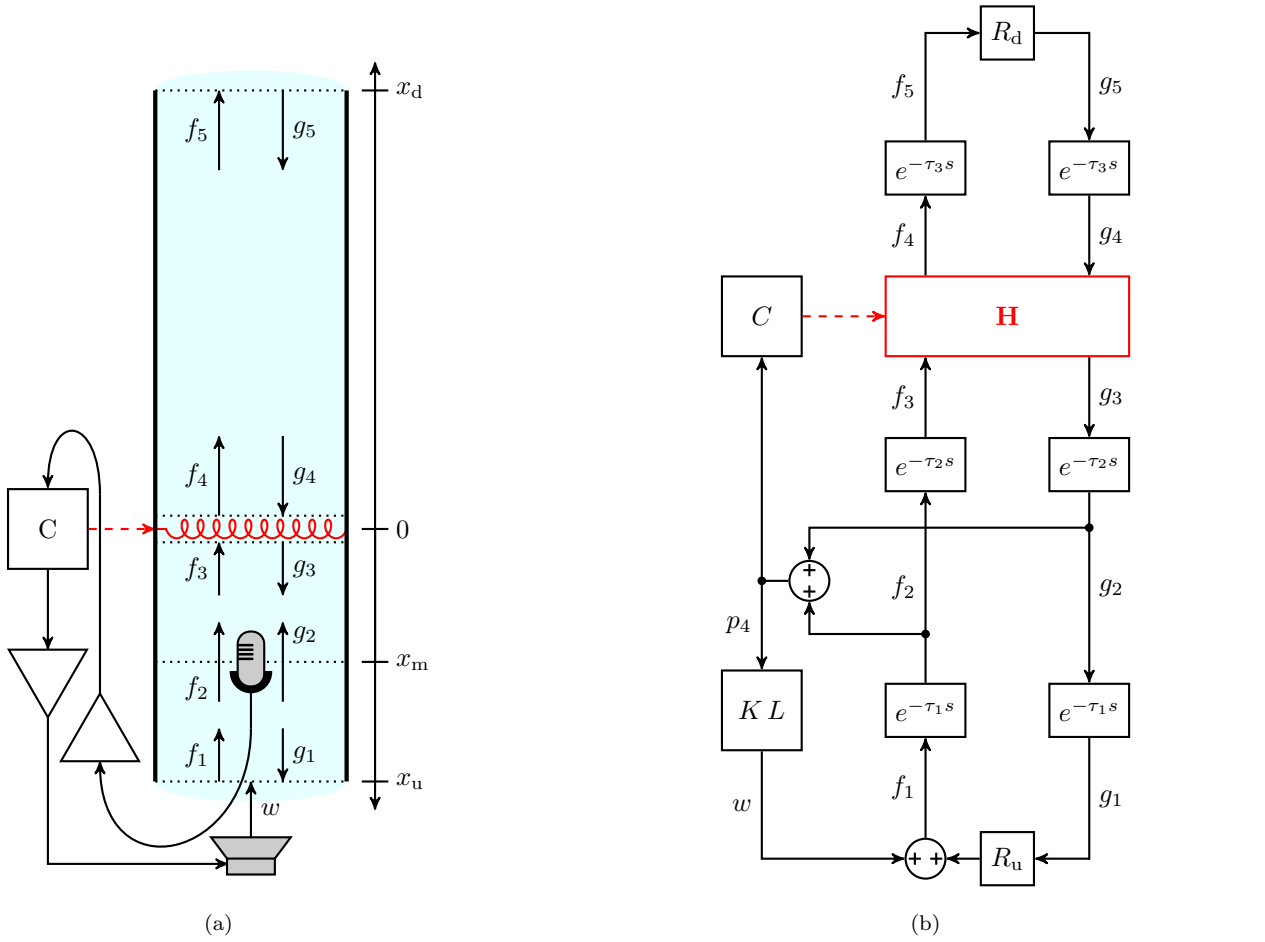

Fig. 1. Simplified time-delay based model of the Rijke tube with a microphone placed below the heater; (a) schematic drawing with highlighted significant cross-sections, (b) block diagram representation

inputs to the system. The heater is explicitly placed close to the lower quarter of the tube length to render the system inherently unstable. The microphone is positioned near the end of the tube, avoiding the position of the acoustic node. We placed the microphone below the heater as oppose to the placement near the farther end of the tube, which appears to be used almost exclusively in the related experiments. Our placement allows for more compact design of the active elements in the tube and also prevents the microphone from being exposed to hot airstream. More on the the effects of this choice on the system can be found in (Pučejdl, 2019).

The modelling assumptions are (i) a stable buoyancy-driven mean upward airstream in the tube with the velocity small compared to the speed of sound, (ii) one-dimensional propagation of both the mean airflow and the acoustic waves along the length of the tube, (iii) negligible thickness of the heater zone, and (iv) no energy dissipation other than the losses due to acoustic reflections at the open ends of the tube, the key modeling concept is the general form of d'Alembert solution of the linear wave equation for acoustic pressure and velocity fluctuations $\tilde{p}$ and $\tilde{u}$:

$$\tilde{p}(x,t) = f\left(t - x/\bar{c}\right) + g\left(t + x/\bar{c}\right), \tag{1}$$

$$\tilde{u}(x,t) = \frac{f\left(t - x/\bar{c}\right) - g\left(t + x/\bar{c}\right)}{\bar{\rho}\bar{c}}, \tag{2}$$

where $\bar{\rho}$ and $\bar{c}$ are the mean air density and speed of sound. Acoustic pressure at each point along the length of tube can be expressed as a combination of two opposing *traveling waves* f and g. Neglecting losses, these travelling waves evaluated in different positions along the tube length are related through *time delays*; on the open tube ends the waves reflect and travel back with the amplitude and phase shift characterized by a *reflection coefficient* (a *reflection transfer function* in the linear case). By evaluating the travelling waves f and g at selected important cross-sections of the tube and defining the respective time delays between these sections, we can translate the spatially distributed problem into a time-delay system. The important sections are the heater zone, the microphone zone, and both ends of the tube. Respective time delays τ_i correspond to the travel times for the acoustic wave between significant cross-sections, hence $\tau_1 = (x_\mathrm{m} - x_\mathrm{u})/\bar{c}$, $\tau_2 = -x_\mathrm{m}/\bar{c}$ and $\tau_3 = x_\mathrm{d}/\bar{c}$.

A block diagram corresponding to such a model in the complex frequency domain is in Fig. 1b. The travelling waves interacting with the heating zone are governed by the heating zone transfer function $\mathbf{H}$ as

$$\begin{bmatrix} g_3 \\ f_4 \end{bmatrix} = \mathbf{H} \begin{bmatrix} f_3 \\ g_4 \end{bmatrix}, \tag{3}$$

and the incident and reflected waves at the tube ends are related by the reflection transfer function. Both denoted control loops regard the acoustic pressure as the control variable. The acoustic control loop contains the controller transfer function K and transfer function L characterizing the microphone, the loudspeaker, and their respective amplifiers. Proper description of the control input from the heater controller C to the system is given in Section 2.1, hence the dashed line in the diagram.

Under the assumptions of linearity and time-invariance (LTI) of the heater, reflection and controller transfer functions, this system fits the LTI time-delay system framework, which allows for some methods of modal analysis as shown by Zalluhoglu and Olgac (2018). Unfortunately, for the purposes of this paper, these assumptions are unrealistic. We aim to use the heater power as the control input; hence, $\mathbf{H}$ is altered artificially in time. Moreover, the heat transfer depends on the heater temperature and airflow velocity, none of which can be assumed constant during experiments, and as we show in the following section, the dependency is also nonlinear.

2.1 Nonlinear Heat Release Model

The linearized version of the heater transfer function can be described as

$$\mathbf{H}(s) = \frac{1}{s + Z_1 + Z_2} \begin{bmatrix} Z_1 & s + Z_1 \\ s + 2Z_1 + Z_2 & -Z_1 \end{bmatrix}, \quad (4)$$

with the coefficients

$$Z_1 = \frac{a(\gamma - 1)}{2Ab\bar{c}^2\bar{\rho}} \quad \text{and} \quad Z_2 = \frac{1}{b}, \quad (5)$$

where b is the time constant of the heat release dynamics, a corresponds to its DC gain, A is the cross-sectional tube area, and γ is the adiabatic ratio. Eq. (4) is borrowed from Zalluhoglu and Olgac (2018) and the form of coefficients in Eq. (5) is broadly accepted in other relevant sources. The core elements to the heat transfer are the effective heat gain represented by a and then first-order lag dynamics based on the boundary-layer effect of thermal inertia (Epperlein et al., 2015).

To obtain an equation for the heat transfer gain a we consider the heat power transfer Q of a hot circular wire in a colder fluid, which is approximately given by King's law

$$Q = f(u_\mathrm{h}) = l_\mathrm{w} \left(\kappa + \kappa_u \sqrt{|u_\mathrm{h}(t)|}\right) (T_\mathrm{w} - T_\mathrm{gas}), \quad (6)$$

where l_w is the length of the heater wire, κ is the fluid's thermal conductivity, κ_u is an empirically determined constant and $u_\mathrm{h}(t)$ is the velocity of the gas at the heater cross section (Vessot and Turner, 1914). The velocity $u_\mathrm{h}(t)$ is given by acoustic velocity fluctuations $\tilde{u}(x_0,t)$ at the heater cross section and the velocity $u_\mathrm{b}(t)$ of the buoyancy-induced convection flow, such that

$$u_\mathrm{h}(t) = \tilde{u}(x_0,t) + u_\mathrm{b}(t). \quad (7)$$

Assuming $u_\mathrm{b}(t)$ positive, yet small, we can write the linear approximation of $f(u_\mathrm{h})$ w.r.t the fluctuating component as

$$g(u_\mathrm{h}) = f'(u_\mathrm{b}(t))\tilde{u}(x_0,t), \quad (8)$$

and the slope of this function corresponds to the heat transfer gain a, hence $a \approx f'(u_\mathrm{b}(t))$. Clearly, it is only when we assume the wire temperature T_w and gas temperature T_gas as well as the mean flow velocity to be constant and velocity fluctuations small, that we can consider Q and a respectively to be constant as well.

Such assumptions can no longer be held when we step out of the frequency-domain and consider the evolution of the Rijke tube behavior in time. Dropping the assumptions results in a becoming a time-varying parameter $a(t)$ as a nonlinear function of the velocity and possibly also a linear function of wire and gas temperature. Moreover, the wire temperature T_w is also influenced by the velocity of the gas, which further complicates the coupling between the variables. We neglect the other possible dependencies (such as the overall temperature increase over time as the tube itself absorbs the heat) and consider the heat release gain to be

$$a(t) = a(u_\mathrm{b}, \Delta T_\mathrm{w}) \approx C_1 \left(1 + \frac{C_2}{2|u_\mathrm{b}(t)|^{3/2}}\right) \Delta T_\mathrm{w}(t), \quad (9)$$

where $C_1 = l_\mathrm{w}\kappa$ and $C_2 = \kappa_u/\kappa$ are constants and $\Delta T_\mathrm{w}(t) = T_\mathrm{w}(t) - T_\mathrm{gas}$ is relative temperature of the wire w.r.t. the temperature of the surrounding gas and environment, which we take as a constant reference point. $\Delta T_\mathrm{w}(t)$ is proportional to the energy which is the integral of the difference of electrical power supplied to the wire and the heat power transferred to the flowing air, hence

$$\Delta T_\mathrm{w}(t) \propto E_\mathrm{w} = \int R(\Delta T_\mathrm{w}) i(t)^2 - Q(u_\mathrm{h}, \Delta T_\mathrm{w}) dt, \quad (10)$$

with $i(t)$ being electrical current flowing through the wire and $R(\Delta T_\mathrm{w}) = R_0 (1 + \alpha \Delta T_\mathrm{w}(t))$ is the temperature dependent electrical resistance of the Kanthal wire, with $\alpha \approx 5 \times 10^{-5}\,1/\mathrm{K}$. Next, using Eq. (9) in Eq. (10), adding the proportionality constant C_3 and differentiating the result, we obtain an affine first order differential equation for ΔT_w with nonlinear time-varying terms in $i(t)$ and $u(t,x_0)$

$$\begin{aligned} \Delta \dot{T}_\mathrm{w}(t) = C_3 \Big\{ & R_0 i(t)^2 + \Big[R_0 i(t)^2 \alpha \\ & - C_1 \left(1 + C_2 \sqrt{|u_\mathrm{h}(t)|}\right) \Big] \Delta T_\mathrm{w}(t) \Big\}. \end{aligned} \quad (11)$$

The Equation (11) describes the dynamics of the wire temperature with the heatercurrent $i(t)$ being the control input to the system. Fig. 2 shows the block diagram implementation of this dynamics as it is later used in the complete model.

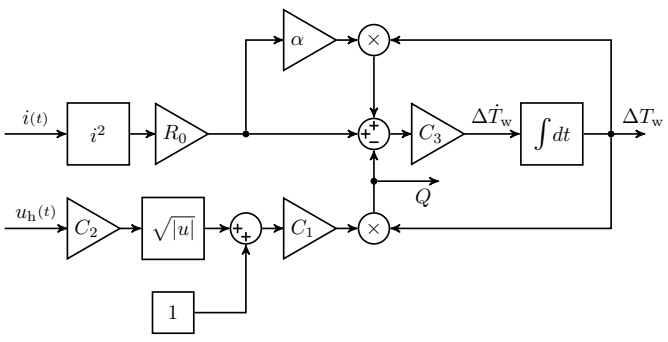

Fig. 2. Block diagram of the wire temperature model

The acoustic velocity fluctuations are easy to obtain from Eq. (2), given the knowledge of the functions $f(t-x_0/\bar{c})$ and $g(t-x_0/\bar{c})$, which we can directly obtain from the simulation model based on the diagram in Fig. 1b.

Considering the dynamics of $u_\mathrm{b}(t)$ is fundamental for capturing the time-domain character of the system, including the attack and decay of the acoustic instabilities. We approximate its behavior with a simple 2nd order system [1], representing some virtual inertia m of the air column and damping ζ caused by viscous friction in the tube and even more so the damping effects at the tube ends.

$$C_4 Q(t) = m\dot{u}_\mathrm{b}(t) + \zeta u_\mathrm{b}(t)\,. \tag{12}$$

The input to the system is the heat power $Q(t)$, and it is scaled by a constant C_4. The virtual inertia is proportional to the inner volume of the tube, and the damping coefficient is assumed constant. Numerical values of all the parameters are empirically determined based on model experiments such that the system reaches reasonable steady-state velocities ($u_\mathrm{b}(t) \approx 1\mathrm{ms}^{-1}$) for given input current and consequent heat release gain. Eq. (12) yields a simple transfer function

$$H_\mathrm{b}(s) = \frac{C_4}{ms+\zeta}\,, \tag{13}$$

which can be implemented in the model of the time-varying heat gain model as shown in Fig. 3

The final form of the transfer function **H** remains identical to the LTI model, only its parameter $a(t)$ is now time-varying and it is governed by the Equation 9. Simplified block diagram of such a system in Fig. 3 portrays the interesting looped coupling between the velocities and heat release. Block **T** contains the nonlinear function from Fig. 2 and block A contains Eq. (9).

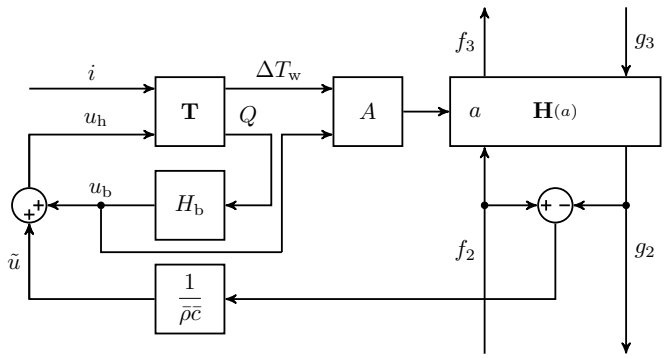

Fig. 3. Block diagram of the time-varying heat transfer

2.2 Acoustic Reflections

Acoustic reflections are critical to forming the standing wave in the tube. The wavelength of the fundamental acoustic mode of the open resonant pipe equals approximately [2] to twice the length of the tube. This fundamental mode at the frequency f_0 dominates over the higher harmonic frequencies due to its lowest attenuation during the acoustic reflections. According to the thorough study by Levine and Schwinger (1948), the reflection behavior corresponds to a linear phase filter that delays each frequency component of the signal by the same fixed amount commonly referred to as a group delay. We decided to model the reflection by a DC gain $-|R_\mathrm{r}(f_0)| \approx -0.95$ and a 1st order Low-Pass filter with a cutoff frequency at $10f_0$. Such implementation does not feature a linear phase response, yet the most important aspect concerning the attenuation of the higher frequencies is included. More in depth explanation of the modeling and obtaining the specific coefficient values is given in (Pučejdl, 2019).

[1] 1st order in velocity.

[2] The actual wavelength needs to be adjusted with so-called *end correction*, which is considered proportional to the pipe diameter.

3. MODEL VERIFICATION AND EXPERIMENTS

To simulate the system we used a Simulink diagram that corresponds to the model in Fig. 1b extended with the nonlinear dynamics in Fig. 3. Most of the numerical parameters in the model relate to the physical properties of the tube or known physical quantities, with the exception of the parameters C_{3-4} and ζ, which we tuned empirically. Due to the coupling effects of several different dynamical models, and a lack of precise dynamical measurements of the temperature and airflow, we were unable to conduct more rigorous system identification. Fig. 4 shows the development of the oscillations when a constant power is supplied to the heater, and there is small initial condition representing some movement of the air in the tube. Buoyant airstream velocity and the temperature of the heater develop and according to expectations.

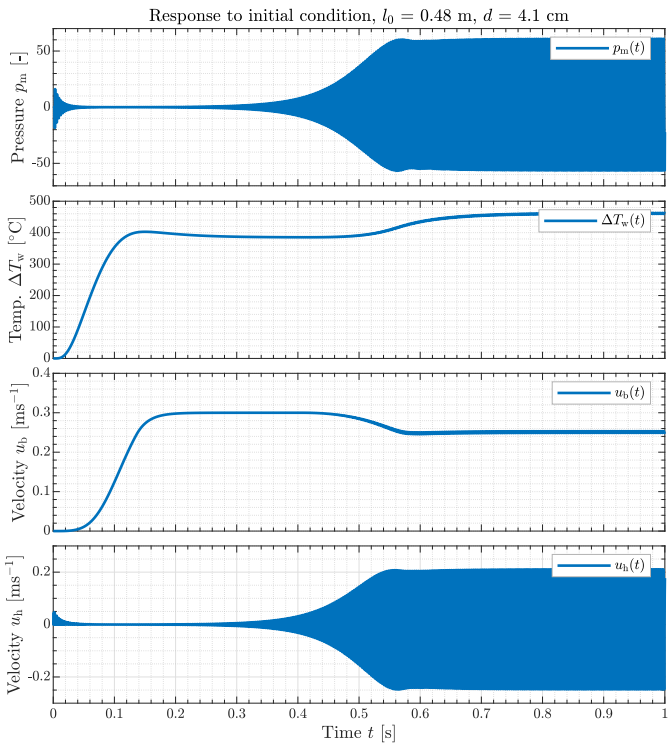

Fig. 4. Tube model response to small initial sound pressure disturbance

.

The FFT analyzed frequency spectrum of the sound pressure signal plotted in Fig. 5 confirms that the system oscillates at the frequency closely matching the expected frequency f_0 determined by the length l of the tube. The

presence of lower gain higher harmonic components in the spectrum also complies with the expectation. Fig. 6 shows the comparison of the short segment of the oscillating waveform obtained from the simulation and the real sound pressure signal measured on the actual Rijke tube with corresponding parameters.

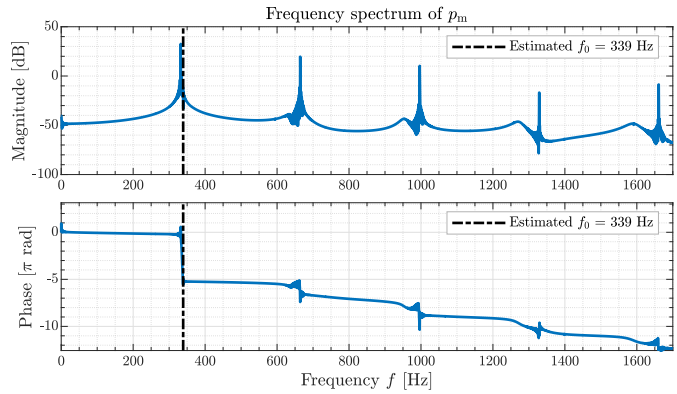

Fig. 5. Frequency spectrum of the sound pressure signal

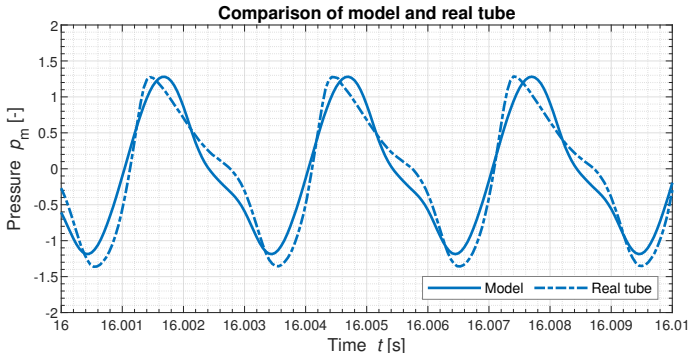

Fig. 6. Close comparison of the simulated waveform and a signal measured on real Rijke tube

4. HARDWARE AND CONTROL SYSTEM

For hardware development and testing the controllers, we built a prototype platform based on a single Rijke tube (see Fig. 8a). The design and construction of the components—the heater element and the microphone in particular—was subject to the general design intent of building the full instrument, which brought several challenges and required custom solutions (i.e. the heater elements and microphones). Upon this platform, we tested and tuned two control strategies, which were previously designed using the mathematical model. This section is just a brief summary and reader is referred to Pučejdl (2019) for more details about the fabrication of the components and specifics of the control system implementation.

4.1 Control system

We specified two main control objectives for enhancing the acoustic performance of the tube. First, we wanted to accelerate the rise and the decay of the tone, which would allow us to trigger the tones more precisely. Second, we needed an amplitude control to be able to play a stable tone and adjust its volume. We use both system inputs—the acoustic input from the speaker and the heat power input from the heater—in either feedback or feed-forward mode. Acoustic feedback stabilization via the time-shifted proportional controller is used for muting the tone and for suppressing the spontaneous rise of the oscillations in the tube, allowing the *idle power* to be provided by the heater. As such, we maintain the buoyant airstream in the tube, which significantly shortens the rise time for the tone. For the tone to be triggered, a short, low-amplitude feed-forward acoustic pulse is used to excite the oscillations, and the heater control switches to the feedback mode to reach and maintain the desired amplitude for the duration of the tone. Observing the first plot in Fig. 7, we can see that the system can track a sequence of 1 second long pulses of varying amplitude. For comparison, an identical tube with simple on-off heating takes several seconds to develop the tone after the heating is turned on, and usually even longer to decay. The tone is not completely muted between the pulses, which is partially caused by the idle current supplied in these time periods; hence, there is a tradeoff between the rise and decay times. Better control strategies could be developed using the offline control input optimization when the reference signal is known prior (e.g., playback music).

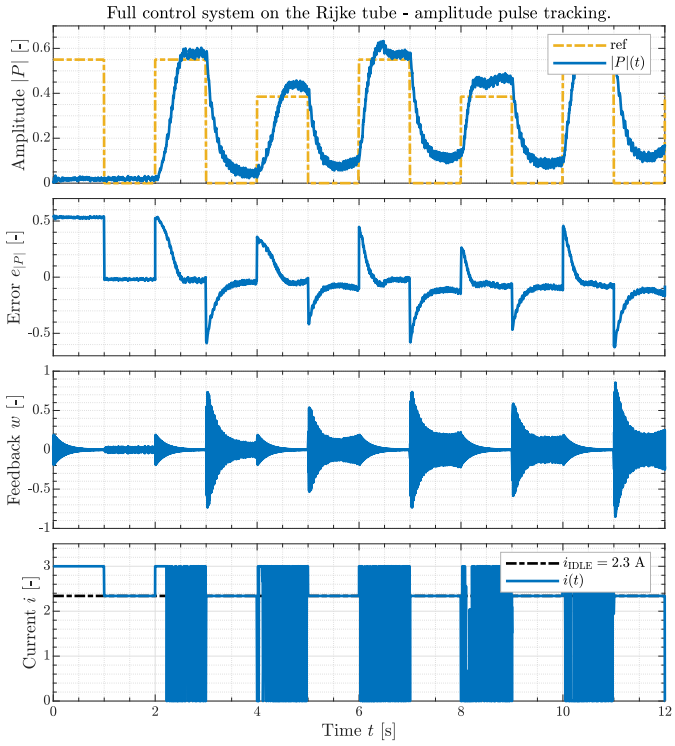

Fig. 7. Amplitude reference tracking using heater current and speaker signal as control inputs

4.2 Rijke Organ

The design of the full Rijke organ was driven by the idea of using a single loudspeaker as an input for multiple Rijke tubes. LTI system with multiple modes can be stabilized by single input if such is able to excite each unstable mode sufficiently and if all of the unstable modes have different natural frequencies. Applicability of this theoretical result

on the nonlinear system consisting of multiple Rijke tubes is not self-evident. The condition of different natural frequencies is sufficed for different lengths of the tubes, but the existence of actuation limits in terms of the maximum power output of the loudspeaker, as well as the nonlinear effects from the tube dynamics, threaten to degrade tge performance. However, our simulations of the mathematical model with two tubes suggested that such an approach should be feasible, and we later confirmed that by the experiments with the real instrument.

We decided to build the first iteration of Rijke organ with 11 borosilicate glass tubes covering tones ranging from F^3 ($\sim$ 174 Hz) to C^5 ($\sim$ 523 Hz), rendering the tallest tube approximately 1 m, and the shortest tube 30 cm tall. The circular arrangement was chosen to utilize the single speaker placed in the middle, approximately 5 cm below the bottom ends of the tubes. The frame is built using predominantly laser-cut plywood and 3D printed parts. Function of the instrument is presented in video clip available at `youtu.be/J1u2lsf7p1Y`.

(a) (b)

Fig. 8. (a) Prototype platform with single Rijke tube and (b) full 11-tube Rijke organ instrument

5. CONCLUSION

We took an unusual perspective when dealing with the physical phenomenon demonstrated by a popular laboratory experiment known as Rijke tube, taking it as a base for a musical instrument. We first developed a mathematical model of the nonlinear dynamics, which features limit cycle oscillations as well as the intertwined dynamics of the buoyant airflow and the heat transfer. This model allowed us to simulate the Rijke tube in time-domain, which is essential for studying the rise and the decay of the oscillations and longer-term effects of the airstream velocity and temperature fluctuations. With this model we tested several control architectures, utilizing both the acoustic control through a loudspeaker placed near the bottom end of the tube and the heat control through a heater placed inside the tube. We built an experimental platform (Rijke tube) and conducted some control experiments. Finally, we extended the setup into a full Rijke organ instrument, featuring 11 individually heated Rijke tubes, all of which are acoustically controlled by a single loudspeaker. We analysed the feasibility of this concept with the simulation model and verified it using the physical experimental setup. One drawback of this setup is the limited power of the speaker. Due to its the placement, a lot of the acoustic power is directed into the void in the middle of the organ column. We also discovered during a public presentation of the organ at *Maker Faire Prague 2019* the sensitivity to the acoustic noise and echo in the room, which is detrimental to the acoustic feedback. The heater control, however, proved to work reliably even in the compromised conditions. To conclude, the instrument proves the concept and offers a solid foundation for continuing developments.

REFERENCES

Campos-Delgado, D., Schuermans, B., Zhou, K., Paschereit, C., Gallestey, E., and Poncet, A. (2003). Thermoacoustic instabilities: modeling and control. *IEEE Transactions on Control Systems Technology*, 11(4), 429–447. doi:10.1109/TCST.2003.810402.

Candel, S.M. (1992). Combustion instabilities coupled by pressure waves and their active control. *Symposium (International) on Combustion*, 24(1), 1277–1296. doi:10.1016/S0082-0784(06)80150-5.

Epperlein, J., Bamieh, B., and Åström, K. (2015). Thermoacoustics and the rijke tube: Experiments, identification, and modeling. *Control Systems, IEEE*, 35, 57–77.

Heckl, M.A. (1988). Active control of the noise from a rijke tube. *Journal of Sound and Vibration*, 124(1), 117–133.

Levine, H. and Schwinger, J. (1948). On the radiation of sound from an unflanged circular pipe. *Physical Review*, 73(4), 383–406.

McManus, K.R., Poinsot, T., and Candel, S.M. (1993). A review of active control of combustion instabilities. *Progress in Energy and Combustion Science*, 19(1), 1–29. doi:10.1016/0360-1285(93)90020-F.

Pučejdl, K. (2019). *Rijke Organ*. Master's thesis, Czech Technical University in Prague, Prague, Czech Republic.

Raun, R.L., Beckstead, M.W., Finlinson, J.C., and Brooks, K.P. (1993). A review of Rijke tubes, Rijke burners and related devices. *Progress in Energy and Combustion Science*, 19(4), 313–364. doi:10.1016/0360-1285(93)90007-2.

Vessot, K.L. and Turner, B.H. (1914). Xii. on the convection of heat from small cylinders in a stream of fluid. *Philosophical Transactions of the Royal Society of London. Series A, Containing Papers of a Mathematical or Physical Character*, 214(509-522), 373–432.

Zalluhoglu, U. and Olgac, N. (2018). Analytical and Experimental Study on Passive Stabilization of Thermoacoustic Dynamics in a Rijke Tube. *Journal of Dynamic Systems, Measurement, and Control*, 140(2), 021007. doi:10.1115/1.4037388.